Effective Dimensions of Oligomers in Size Exclusion Chromatography. A Molecular Dynamics Simulation Study

R. H. Boyd*

Department of Materials Science and Engineering and Department of Chemical Engineering, University of Utah, Salt Lake City, Utah 84112

R. R. Chance and G. Ver Strate

Paramins Technology Division, Exxon Chemical Company, Linden, New Jersey 07036

Received June 20, 1995; Revised Manuscript Received August 7, 1995[⊗]

ABSTRACT: Size exclusion chromatography (SEC) is a widely used method for determining the molecular weights of polymer molecules. SEC calibration is often achieved using the "universal calibration" technique, which assumes hydrodynamic volume is the sole determinate of retention time. Recent work has demonstrated the failure of this approach when molecular weights are small (<5000) and particularly in the oligomer range. In order to explore the theoretical reasons for this failure, molecular dynamics (MD) simulations have been used to compute the partition coefficients as a function of pore size for oligomeric series of three polymers: polyethylene (PE), polyisobutylene (PIB), and polystyrene (PS). The molecular weight ranges studied were from dimers up to 500 g/mol for PE and up to 1000 g/mol for PIB and PS. MD simulation was used to generate a large number of configurations of the various oligomers. These configurations were then used to compute the partition coefficients of the species in cylindrical pores of varying diameters. The MD model of the oligomers included all atoms explicitly and all internal degrees of freedom. Solvent was not included specifically but the configurations were generated under phantom chain conditions for longer range interactions that are appropriate to the Θ solvent conditions that prevail for short molecules. The variation of partition coefficient with pore size for a given oligomer could be described well by assigning an effective hard-sphere radius, called here the retention radius, to the molecule. The retention radii for an oligomer series were found to correlate well with the radii of gyration. There were however significant differences in the retention radii vs radii of gyration correlations among the three series studied. At the same radius of gyration, the retention radii order is found to be PS > PIB > PE. This order agrees with experimental SEC data for retention times for these oligomer series. The differences are attributed to asphericity of individual configurations enhancing the effects of substituent size. The approach of the mean-square radius of gyration and mean-square end-to-end distance dependence on chain length to limiting long-chain behavior is discussed. It is found that the limiting proportionality to chain length has not been reached in the molecular weight ranges studied. A comparison of the use of the intrinsic viscosity−molecular weight product ($[\eta]M$) as a measure of radius of gyration, the radius of gyration determined independently, and the retention radius from simulation as criteria for equal retention times is made. The errors in molecular weight determination resulting from the use of each of the three criteria are discussed. The retention radius from simulation is found to be a significantly better criterion for retention time than the $[\eta]M$ product or directly determined radius of gyration.

I. Introduction

Size exclusion chromatography (SEC) has proven to be an extremely valuable tool in determining molecular weight and its distribution in polymers.[1,2] Although inherently not an absolute method, some simplifications allow its convenient use. Chief among these is the "universal calibration" (UC) method. It is based on the concept that hydrodynamic volume in solution determines the retention characteristics. This volume is taken to be related to the intrinsic viscosity, $[\eta]$, and molecular weight, M, through the Einstein relation that states that $[\eta]$ is proportional to hydrodynamic volume divided by M. Thus the hydrodynamic volume is related to viscosity and molecular weight as the product $[\eta]M$. This relation has been applied to polymers of various overall molecular architectures including linear, branched, graft, comb, and ladder. For the case of linear polymers, the universality of the method parallels the long-held proposition, based on much theoretical work, that the viscosity, $[\eta]$, is proportional to R_g^3/M, where R_g is the radius of gyration and suggests that the constant of proportionality, Φ, is universal. That is, a single value of Φ holds for all linear polymers. Thus a central role for R_g as a universal descriptor of effective molecular size in linear polymers is implied.

Though there is considerable interest in applying SEC to low molecular weight polymers and oligomers, there are problems that arise in applying the UC in this regime. It is well-known that the standard relations, such as the Mark−Houwink equation, between molecular weight and intrinsic viscosity break down at low molecular weight, even to the point of observation of negative values of intrinsic viscosity. Significant deviations from the basic premise that retention is a universal function of radius of gyration also have been found in the oligomer range.[3] This includes whether R_g is from the $[\eta]M$ product, determined from scattering experiments or from rotational isomeric state (RIS) calculations. This latter aspect, the role of R_g in describing effective size in retention, is examined here.

In the present work we use molecular simulations as a means of investigating the relation between retention and molecular size and structure. The strategy is to use cylindrical pores as a model for the retention substrate and to determine via simulation the partition coefficients of molecules in the pores. SEC is normally conducted in a slow flow region where hydrodynamic

[⊗] Abstract published in *Advance ACS Abstracts,* November 1, 1995.

0024-9297/96/2229-1182$12.00/0

factors do not contribute substantially and the separation is dominated by the static partition coefficients. The molecular structures are generated in realistic all-atom detail using molecular dynamics (MD) simulations. Partition coefficients for ranges of both molecular chain length and pore size are computed for a given oligomer family.

Three oligomer families were chosen for study. These are polyethylene (PE), polyisobutylene (PIB), and atactic polystyrene (PS). These three have been the subject of a recent extensive experimental investigation of retention behavior in SEC.[3] PS of course has been the archetypal polymer upon which to base UC procedures.

II. Simulation Methodology

In the work here only the effect of geometrical constraint of the pores and its relation to the conformational and shape properties of the solute oligomers are examined. The solvent is deleted on an explicit basis. The principal effect of solvent is on the relation between root-mean-square end-to-end distance or radius of gyration and chain length. In good solvents the attractive polymer bead−solvent contacts suppress bead−bead self-contacts and cause chain expansion relative to unperturbed conditions. In the high molecular weight limit, the exponent in the coil size vs chain length power law relation approaches $^3/_5$. This corresponds to a value of the Mark−Houwink exponent of $^4/_5$. In Θ solvents, where there is no discrimination against bead−bead contacts, unperturbed or phantom conditions prevail and the exponent takes the classic random walk value of $^1/_2$. The Mark−Houwink exponent takes on the same value. However, in the low molecular weight limit, polymer bead−bead self-contacts become more and more rare solely on the basis of chain lengths being too short to generate many of them. The chains tend toward phantom behavior regardless of solvent quality. Therefore in the low molecular weight regime of interest here, unperturbed or phantom conditions are a reasonable approximation to the real situation.

The cylindrical pore has been used as a model for partitioning in a number of theoretical or simulation studies of idealized molecules.[4−6] Under the above conditions for cylindrical pores, the partition coefficient reduces to the fractional cross-sectional area of the pore available to a molecular configuration averaged over a representative population of configurations of free chains. The interpretation of our simulation results depends heavily on the analogy with the partitioning of hard spheres. The use of the radius of gyration as a measure of size is inherently an expression of this analogy. Thus below we discuss the partition coefficient in this context.

The partition coefficient between a solute (oligomer) in a pore and in the bulk is found by computing the chemical potential of the solute in both states and equating them. In the absence of solvent molecules, the system considered consists of a single component. The configurational (Helmholtz) free energy of the single component system is given by

$$A = -\beta^{-1} \ln Z/N! \tag{1}$$

where the configurational partition function, Z, is

$$Z = \int_V \exp[-\beta \sum_{i>j} U_{ij}(|\mathbf{r}_j - \mathbf{r}_i|)]\, d\mathbf{r} \tag{2}$$

$\beta = (k_B T)^{-1}$, U_{ij} is the potential energy of interaction between particles i and j, and the integration of the positions of all the particles, $\mathbf{r}$, is over the volume, V. The integration over V and its details are at the heart of computing the distribution coefficient.

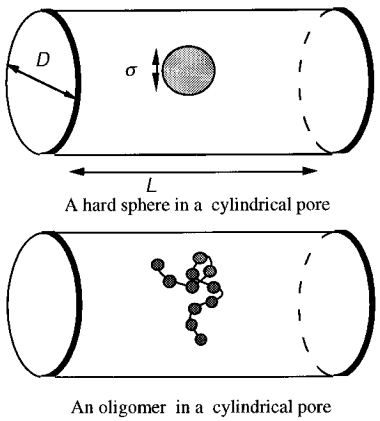

Figure 1. Hard sphere and an oligomer in a cylindrical pore, the geometry adopted for representing the porous substrate.

Consider, by way of instructive example, the simple case of a collection of hard spheres in a cylindrical pore of considerable length (see Figure 1). Further, consider the limit of very few spheres in the pore so that they do not interact with each other. Then the energy term U_{ij} may be taken as zero between spheres, and only the effect of the pore wall is considered. The partition function is just the integral of d$\mathbf{r}$ of the center of each sphere over the pore volume. Thus for N spheres of diameter σ in a long pore of diameter D and length L and with volume $V = \pi(D/2)^2 L$

$$Z = [(\pi/4)(D - \sigma)^2 L]^N = V^N[(1 - \sigma/D)^2]^N \tag{3}$$

The configurational contribution to the chemical potential, μ, is found from eq 1, using $\mu = (\partial A/\partial N)_{T,V}$, or

$$\mu = -\beta^{-1} \ln[(V/N)(1 - \sigma/D)^2] \tag{4}$$

Let the bulk solution, where $D \rightarrow \infty$, be denoted by superscript zero. Then from $\mu = \mu^0$, the partition coefficient, K, is

$$C/C_0 = K = (1 - \sigma/D)^2 \tag{5}$$

where $C = N/V$ and $C^0 = N^0/V^0$ are the concentrations in the pore and bulk, respectively. Thus it is especially transparent that the partition coefficient decreases as the size of the molecule approaches the diameter of the pore.

Now consider the more complicated case of polyatomic molecules (see Figure 1). The molecules in the pore are still considered as dilute. Then the configuration integral will still be the product of N identical integrals, one for each molecule or

$$Z = z^N$$

where z is a single-molecule configurational integral given by

$$z = \int_V d\mathbf{r}_0 \int_V d\mathbf{r}_{i0} \exp[-\beta \sum_{i>j} U_{ij}(|\mathbf{r}_{ij}|)] \tag{6}$$

in which $\mathbf{r}_0$ is the position of the center of mass (CM) of the molecule, $|\mathbf{r}_{ij}| = |\mathbf{r}_j - \mathbf{r}_i|$ is an *intra*molecular distance, and the sum in the potential energy is over

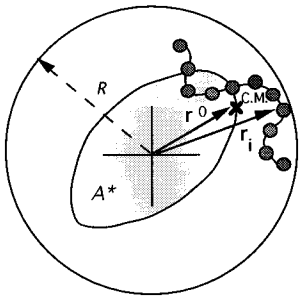

Figure 2. Oligomer of a given configuration (conformation) in a pore. The center of mass (CM) vector, $\mathbf{r}_0$, sweeps out an effective area, A^*, when moved over the cross section of the pore, subject to the constraint of all position vectors, $\mathbf{r}_i$ (plus van der Waals radius), lying inside the pore radius, R. The process is repeated for many configurations generated from MD in order to find an average A^* to be used in eq 7 for the distribution coefficient.

all such interactions. The integration $d\mathbf{r}_{i0}$ is over the atom coordinates relative to the CM. Consider a volume so large that the integration over the internal coordinates generates a Boltzmann-weighted population of *free* chains. In a hard wall confinement, for a fixed value of the center of mass vector, integration over the internal coordinates is equivalent to selecting from the population of free chains those that do not impinge on the pore wall. Subsequent integration of the center of mass vector over the confined volume generates a volume weighted by the number of acceptable configurations. In simulation, this can be reproduced by first generating a representative population of free chains and then determining the volume available to each member of the population.

Employment of molecular dynamics, MD, for an isolated chain will generate a trajectory that consists of a series of configurations over time that fairly represents the desired Boltzmann weighted configurations. The CM of a configuration from the population is moved over the cross section of the pore, subject to the constraint that no part of the molecule (including van der Waals spheres about the atoms) can penetrate the wall. This is completely analogous to the hard-sphere integration above, eq 3. Just as for the hard spheres, part of the pore area will be inaccessible. This process determines an available cross-sectional area, A^* (see Figure 2). The partition coefficient will be given by

$$K(R) = A^*(R)/\pi R^2 \tag{7}$$

where $A^*(R)$ is the cross-sectional area of a pore radius R available to the oligomer.

The above procedure is rigorous within the assumptions of the model. To recapitulate, the assumptions are that the pore is a long, hard cylinder, that the solvent interactions can be omitted and phantom chain conditions invoked, that the intramolecular potential energy function parameters in the MD simulation are adequate, and that the MD is carried out long enough to generate a representative set of conformations.

III. Simulation Details

The general MD methods used by us for bulk systems have been described previously.[7−9] Single-chain conditions were invoked here by use of a very large periodic box size. In the present work the use of explicit hydrogen atoms occasioned the use of a smaller time step, i.e., 0.5 fs. The potential function parameters were taken from the MOLBD3 force field.[10,11] The bond-stretching constants were reduced by a factor of 4 in order to lengthen the time step. The parameters are listed in Table 1. Constant-temperature runs were made via the Nosé[12] extended system method.

Table 1. Potential Function Parameters[a]

Nonbonded Functions: $V(R) = A\exp(-BR) - C/R^6$

atom types[b]	A	B	C
H H	11089	3.74	114.50
C H; CA H	18079	3.415	578.53
C C; CA CA; C CA	62675	3.09	2681.7

Bond Stretch: $V(R) = {}^1/_2K(R - R_0)^2$

atom types	K	R_0
C C	641.8	1.53
CA C	641.8	1.50
CA CA	1130	1.39
C H	678	1.09
CA H	678	1.09

Bond Bend: $V(\theta) = {}^1/_2K(\theta - \theta_0)^2$

atom types	K	θ_0
C C H	359.1	1.9106
H C H	322.2	1.8832
CA C C	447.8	1.9373
C C C	447.8	1.9373
CA CA C	418.5	2.0945
CA C H	334.8	1.9106
CA CA CA	602.6	2.0945
CA CA H	322.2	2.0945

Torsions:[c] $V(\phi) = {}^1/_2V_0(1 + C\cos N\phi)$

atom types	V_0	N	C
C C C C	10.46	3	1
C C C HM[d]	10.46	3	1
CA CA C C	0.21	3	1
CA CA CA C	54.4	2	−1
CA CA CA CA	108.8	2	−1
CA CA CA H	54.4	2	−1

[a] Energies are in J/mol, distances in Å, and angles in radians. [b] Atom types: "C" = aliphatic carbon; "CA" = aromatic carbon; "H" = hydrogen; "HM" = terminal hydrogen. [c] One torsion is set up for each atom type sequence. Thus, for example, there are two CA CA CA H torsions for each aromatic ring hydrogen. [d] All main-chain torsions are in C C C C. No torsions are included for the main-chain sequences H C C H and C C C H. However, at each of the two terminal main-chain torsions it is necessary to invoke one hydrogen. This is designated as C C C HM.

One polymer chain was used to represent each set of oligomers. For example, a polyethylene chain of formula $H-(CH_2CH_2)_{18}-H$ was constructed and subjected to MD runs. Phantom chain conditions were enforced by omitting nonbonded interactions between centers whose atom numbers, under a system in which the latter (including all substituent atoms in the repeat unit) increase sequentially along the chain, differ by more than 15. This number is selected to be big enough to make sure that all nearby interactions such as those that lead to gauche−trans energy differences and four-bond steric interferences are included. For this one chain several long MD trajectories were generated. Sampling of configurations was carried out at intervals along the trajectories. For each of these sampled configurations, the integration over the pore cross section to determine A^* in eq 7 was carried out. In doing so, each of the smaller oligomers $n = 4, 6, 8, ..., 18$ were also computed by regarding one end as the beginning of the chain and including the only first n CH_2CH_2 units in the calculation. Since phantom conditions were invoked, this procedure is appropriate. In

Table 2. Simulation Summary

oligomer series	temp (K)	total trajectory, steps[a]	main-chain conf transitions[b]
polyethylene $H-[CH_2CH_2]_n-H$, $n = 2, 4, 6, ..., 18$	300	4M	1975
polyisobutylene $H-[CH_2C(CH_3)_2]_{18}-H$, $n = 2, 4, 6, ..., 18$	350	10M	405
polystyrene[c] $H-[CH_2CH(phenyl)]_n-H$, $n = 2, 3, 4, ..., 10$			
PS-1 mrrmmrrmm	375	1580K	170
PS-2 mrrrrrmrm	350	1M	87
PS-3 rrmrrmrrm	350	1100K	89
PS-4 rmrmmrrmr	350	2300K	123

[a] Each step is 0.5 fs. [b] Number of transitions in the complete chain, i.e., for the maximum n value. Based on $2n - 3$ bonds. [c] Four molecules were studied; the diad contents are shown; m = *meso*, r = racemic.

the A^* integration van der Waals spheres of radius 1.50 Å were inscribed about hydrogen atoms and radius 1.725 Å about the carbon atoms. In carrying out the A^* integration, the sampled configuration was introduced into the pore in each of three different orientations, with the molecule x, y, or z axes along the pore cylindrical axis. Since the configurations tend to be elongated, this improves the integration statistics. The square of the radius of gyration, R_g^2, and the square of the end-to-end distance, R^2, were also calculated for each of the oligomeric lengths within each sampled configuration.

For PIB the chain considered was $H-[CH_2C(CH_3)_2]_{18}-H$. Most of the experimental data are on PIB with olefin end groups. In the case of dimer we found that the elution times of structures with and without the double bond were the same within experimental error, and thus this is not an issue in comparing the simulations and experiments. For polystyrene the chain contained 10 monomer units with −H terminations. Since in practice the polystyrenes of interest are atactic, a group of chains with diad contents with overall *meso* probability of 0.43 was generated.[13] From this group the first four chains were selected and MD trajectories generated for each. The structures were designated as PS-1 through PS-4. The diad contents of these are shown in Table 2. More chains were not included because the simulations showed the retention behavior was not significantly different among the members of this limited sample. The atom number offset for nonbonded interaction omission was >48 for both PIB and PS. These offsets ensure that all interactions between a monomeric unit and the next 3 monomeric units are included for PIB and the next 2 for polystyrene.

The lengths of the trajectories were governed by the requirement of generating a representative set of conformations. The ultimate test of this is the stability of averages to longer and longer runs. A useful shorter term monitor of the ability to achieve equilibration is the rate at which conformational transitions occur. A number of transitions at each main-chain bond should accumulate. It appears that than an average of 5−10 transitions per bond results in equilibration of properties. The lengths of the trajectories and the number of transitions observed are shown in Table 2. The radius of gyration involves sums over all of the atom pairs present. This is in contrast to the end-to-end distance, which involves only the end atoms. Thus the statistics and convergence of averages for the former are better than for the latter, especially as chain length increases.

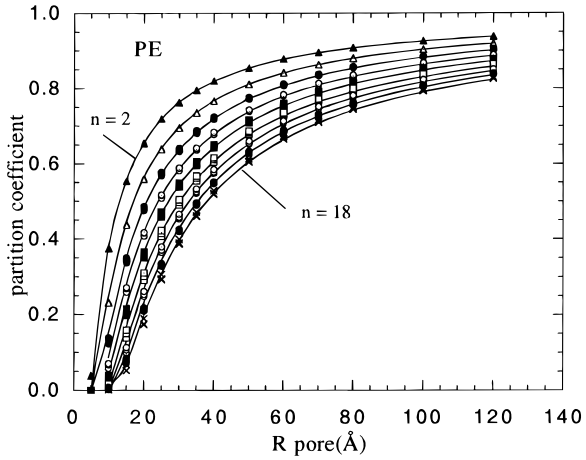

Figure 3. Partition coefficient as a function of pore radius as determined from simulation. The points are for oligomeric polyethylenes (PE) of n-mer range $n = 2, 4, 6, ..., 18$. The solid curves were calculated from the retention radii, R_{ret}, determined in Figure 6 using eq 9.

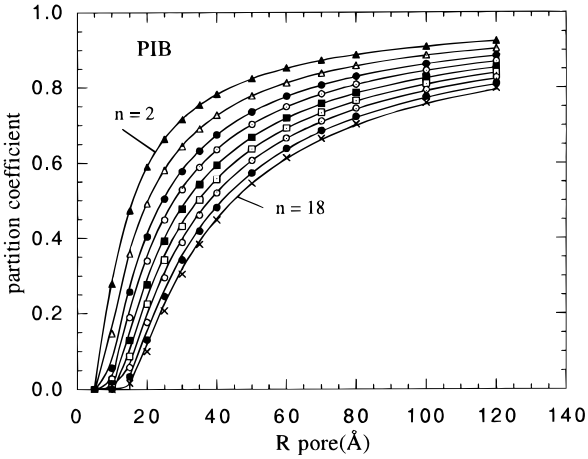

Figure 4. Partition coefficient as a function of pore radius as determined from simulation. The points are for oligomeric polyisobutylenes (PIB) of n-mer range $n = 2, 4, 6, ..., 18$. The solid curves were calculated from the retention radii, R_{ret}, determined in Figure 7 using eq 9.

IV. Results and Discussion

Plots of the partition coefficient as a function of pore size at each oligomer size are shown for PE in Figure 3, for PIB in Figure 4, and for PS-1 in Figure 5.

Effect of Pore Size and Definition of a "Retention Radius". For the case of hard spheres, an explicit relation (eq 5) connects the partition coefficient at various pore sizes with a single parameter, the sphere diameter. This suggests invoking the following procedure in order to simplify the interpretation of the above curves. An effective hard-spheres radius for an oligomer is calculated at each pore size by inverting eq 5, that is,

$$r_{\text{hard sphere}} = R_{\text{pore}}(1 - K(R_{\text{pore}})^{1/2}) \qquad (8)$$

The results of this exercise for the three sets of curves in Figures 3−5 are shown in Figures 6−8. It may be seen that the effective molecular radius at a given oligomer length does approach constancy fairly quickly as pore size increases. To take advantage of this, an effective molecular *radius for retention*, R_{ret}, has been

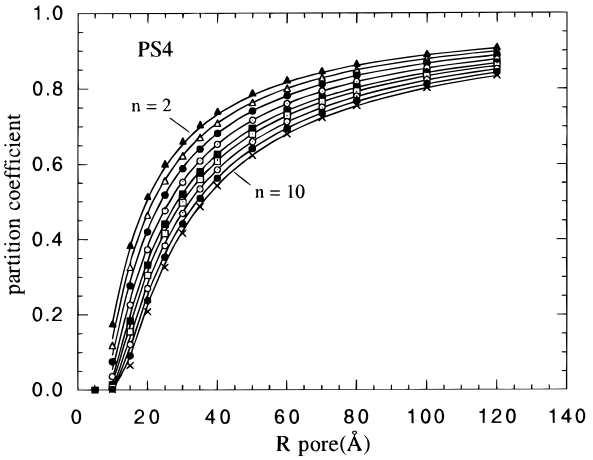

Figure 5. Partition coefficient as a function of pore radius as determined from simulation. The points are for oligomeric polystyrenes (PS) of *n*-mer range $n = 2, 3, 4, ..., 10$. The solid curves were calculated from the retention radii, R_{ret}, determined in Figure 8 using eq 9.

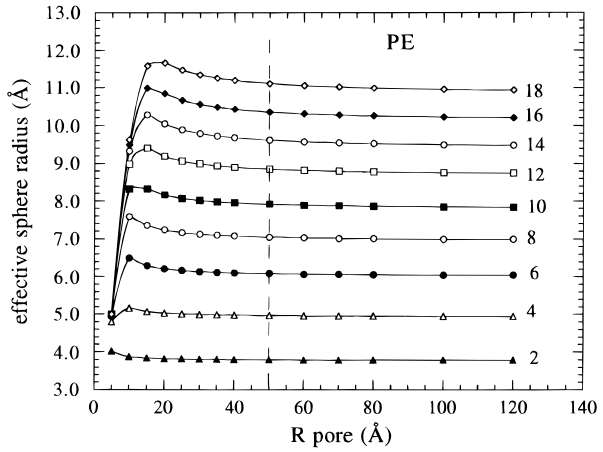

Figure 6. Determination of an effective hard-sphere radius for each oligomer, *n*, for PE. Each point is calculated from the corresponding point in Figure 3 using eq 8. The effective *retention radius*, R_{ret}, is defined as the value at 50 Å for each oligomer (as indicted by the vertical dashed line). The curves shown connect the data points for clarity.

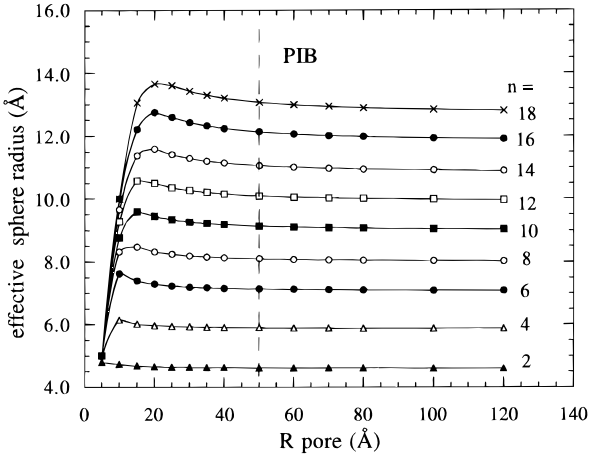

Figure 7. Determination of an effective hard-sphere radius for each oligomer, *n*, for PIB. Each point is calculated from the corresponding point in Figure 4 using eq 8. See Figure 6.

defined here as the hard-sphere radius calculated from eq 8 at $R_{pore} = 50$ Å. The R_{ret} values are indicated in Figures 6−8 by the intersections of the vertical dashed lines at 50 Å with the curves. In verification of the

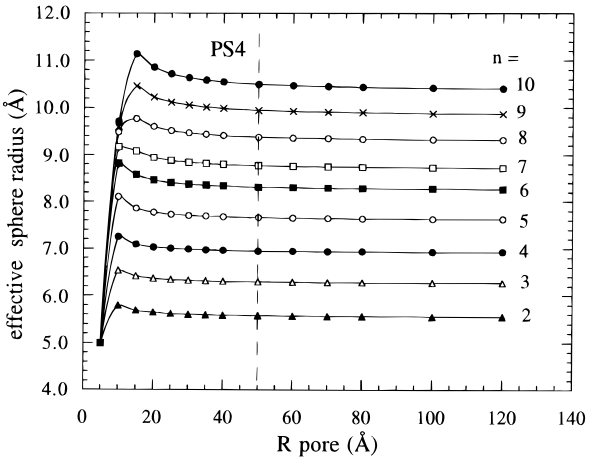

Figure 8. Determination of an effective hard-sphere radius for each oligomer, *n*, for PS-4. Each point is calculated from the corresponding point in Figure 5 using eq 8. See Figure 6.

effectiveness of this procedure, the partition coefficient as a function of pore radius may be calculated from

$$K(R_{pore}) = (1 - R_{ret}/R_{pore})^2 \qquad (9)$$

and compared to the actual values determined from simulation displayed in Figures 3−5. The curves in these figures were determined from eq 9 using the R_{ret} values determined in Figures 6−8. It may be seen that the fits to the simulation data are excellent.

The retention radius R_{ret} thus summarizes very well the partition coefficient behavior of a given oligomer. The larger the value of R_{ret}, the smaller will be the partition coefficient and hence the shorter the retention time. Because the partition coefficient depends on the *square* of one minus the ratio of the effective radius to the pore radius, modest differences in retention radii can be significant with respect to retention.

Correlation of Retention Radius with Radius of Gyration. As indicated in the Introduction, the hydrodynamic volume, i.e., the $[\eta]M$ product, is the most widely invoked concept in the interpretation of SEC. For linear polymers the radius of gyration R_g can be inferred from the $[\eta]M$ product. Values can also be directly determined from scattering experiments and from rotational isomeric state calculations. In particular, there are some experimental values of R_g available for PS and PIB as has been previously discussed.[3] In this work, values of R_g were accumulated in the simulations in addition to the partition coefficient results. The simulation values are compared with the experimental ones in Figure 9. The data are from Chance et al.[3] and Einaga et al.[13] The agreement seems satisfactory.

The universality of the relation between partition coefficient or retention time and R_g is explored in Figure 10. There the R_{ret} effective retention radii values are plotted against R_g. It may be seen that for each oligomer series a smooth correlation is found. The curves shown are linear fits although for the PS series very slight curvature is evident. These individual correlations are tight in a statistical sense. The effect of variation in R_g, as for example in the variations among the four PS structures, is to move along the curve rather than to introduce scatter.

Thus Figure 10 indicates that R_g is a good measure of effective size *within* a series. However, it is also to be noticed that there are significant differences among the correlations for the three series studied. At the

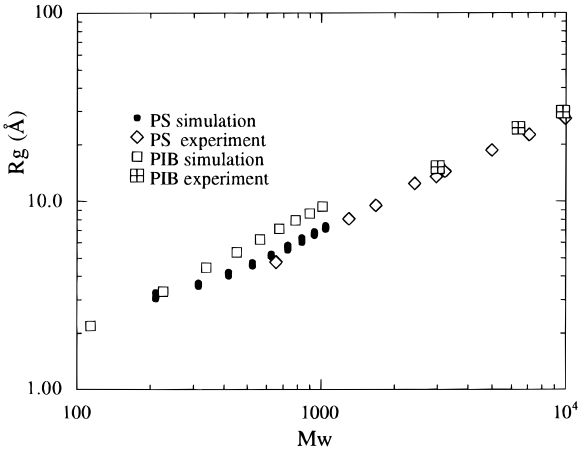

Figure 9. Radii of gyration, R_g, from simulation compared with the experimental values that are available for PIB and PS. Both are plotted against molecular weight (weight average for the experimental values).

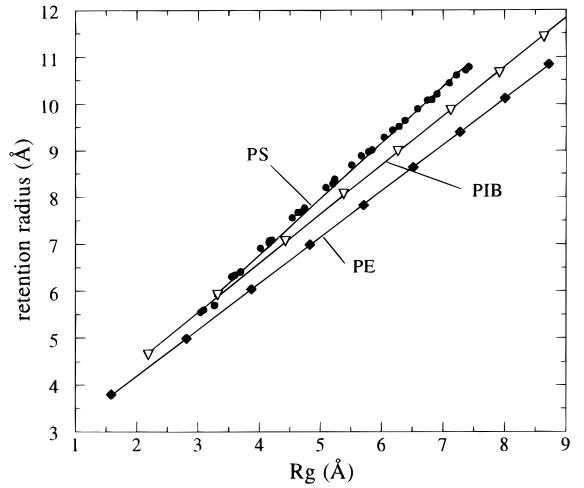

Figure 10. Retention radii for the three oligomer series plotted against the corresponding radii of gyration, R_g.

same radius of gyration, the effective retention radii order is seen to be PS > PIB > PE. Thus the retention times should be in the inverse order. This order was previously observed experimentally.[3] More detailed comparison with experiment is made in the next section.

A word is in order about rationalizing the above result concerning the differences in the retention radii vs radii of gyration correlations for the series studied. The fact that the retention sizes go as PS > PIB > PE at the same R_g must be connected with the sizes of the substituent side groups and the effective molecular cross sections. The radius of gyration is based on a weighted sum of squares of the distances to the center of mass of *all the atoms present* including the side groups and thus to some degree it responds to the effect of the latter. Explicitly,

$$R_g^2 = M^{-1}\left(\sum_i m_i x_i^2 + \sum_i m_i y_i^2 + \sum_i m_i z_i^2\right) \quad (10)$$

where x_i, y_i, and z_i are the coordinates of atom i with mass m_i in a system with origin at the center of mass and M is the total mass.

If individual configurations were spherical, it would be expected that R_g would incorporate the effects of substituent sizes. However, in the range of molecular lengths considered, a typical individual molecular configuration is quite elongated and far from the spherical

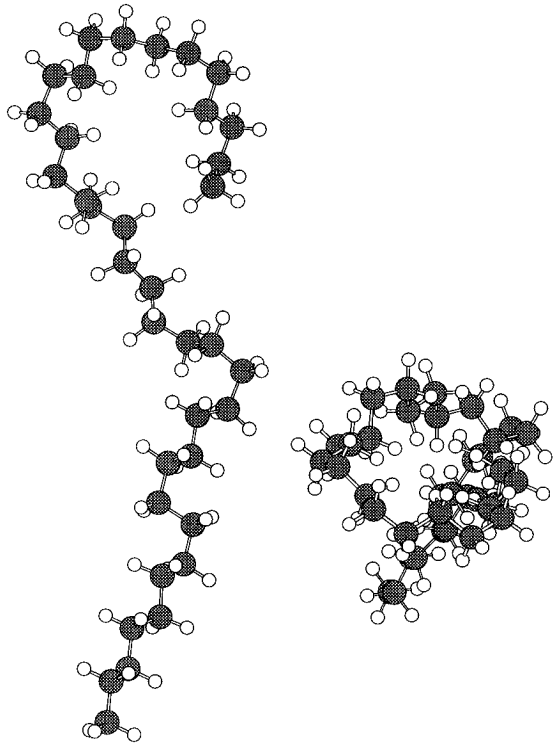

Figure 11. Asphericity of configurations. A configuration of PE, n-mer = 18, from simulation. Two views are shown: one is normal to the most extended direction, and the other one is along it. It may be seen that, even at the longest chain lengths studied, the configurations tend to be elongated. The cross-sectional area normal to the long direction is quite sensitive to the substituents present while the radius of gyration is not. The latter is sensitive to the length in the long direction, and the substituents have little effect on this.

symmetry associated with infinitely long chains (see Figure 11). If such a configuration were to be expressed in terms of its principal inertial axes, one of the principal moments (about the "long" axis) would tend to be significantly smaller than the other two. The relative contributions to the radius of gyration from each of the principal axis directions are quite sensitive to this elongation. The transverse contributions would be diminished compared to that from the long axis. In the limit of long highly extended conformations, R_g will depend only on the molecular length as expressed by the number of chain bonds and not at all on the transverse contribution of substituents. In introducing a configuration into the pore, the molecular long axis will be randomly distributed with respect to the pore cylinder axis. Acceptance depends strongly on the long axis orientation and dimension. R_g is a good measure of this length. The acceptance of the configuration at a given pore radius will obviously be biased toward the molecular long axis being the pore cylinder axis. In turn this implies, among those configurations with proper long-axis orientation, that the role of the molecular cross section in the transverse direction, in achieving acceptance will be enhanced. This cross section, since it is relatively small, will be sensitive to the size of the substituents. As an extreme illustrative example, one could consider the case of two types of molecules that are both very elongated cylinders with the same radius of gyration but with different diameters (substituents). On introducing them into a cylinder pore, since the molecules would have to fit along the cylinder axis, the acceptance would depend entirely on the molecular cross section diameters.

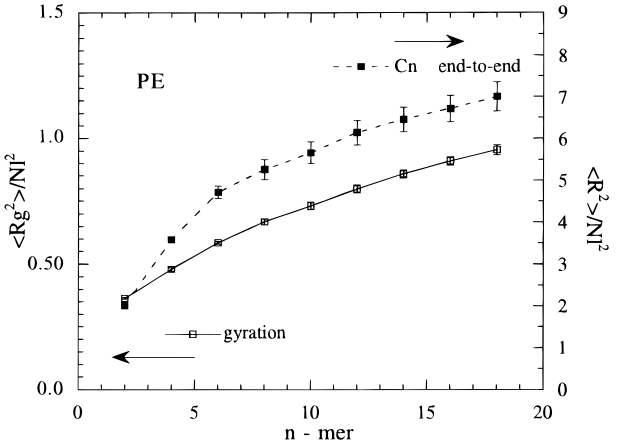

Figure 12. Characteristics ratios for radius of gyration R_g and end-to-end distance, R, plotted against chain length (expressed as n-mer number) for PE. The scale of the radius of gyration (left side) is set at 6 times that for the end-to-end distance (right side) so that they should merge in the high molecular weight limit. The error bars represent the standard deviation of five equal subtrajectories.

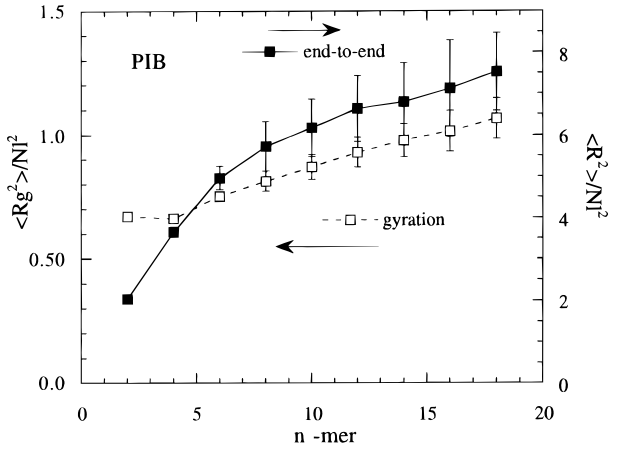

Figure 13. Characteristic ratios for radius of gyration R_g and end-to-end distance, R, plotted against chain length (expressed as n-mer number) for PIB. See Figure 12. The error bars represent the standard deviation of five equal subtrajectories.

In summary, the lack of tight universality of R_g as a retention measure is to be attributed to asphericity of individual configurations at lower molecular weights.

Approach of R_g^2/N to the High Molecular Weight Limit. It is a fundamental property of coiling polymer chains that the mean square radius of gyration under Θ conditions becomes proportional to the molecular length in longer chains.[14,15] Although not of direct consequence in exploring the role of R_g as a descriptor of size in SEC, it is nevertheless of interest to examine this question. The characteristic ratio for the radius of gyration is defined as $S_N = \langle R_g^2 \rangle / Nl^2$, and the characteristic ratio for the end-to-end distance, R, is defined as $C_N = \langle R^2 \rangle / Nl^2$, where in both N is the number of chain bonds and l is the bond length. In general, the approach to the asymptotic limit with increasing N is slower for S_N than for C_N.[14,15] Not only should these quantities approach an asymptotic limit at large N, but their ratio should approach the value 6. Both ratios are plotted against chain length in Figure 12 for PE and in Figures 13 and 14 for PIB and PS, respectively. In Figures 12−14 ratios of the left- and right-hand axes are also chosen in the ratio of 6. Thus the S_N and C_N curves, as plotted, should merge at high N. Except for the first few n-mers where the substituent dimensions are comparable to the

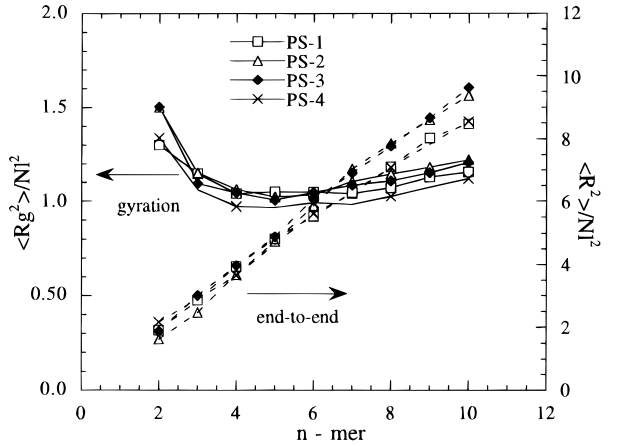

Figure 14. Characteristic ratios for radius of gyration R_g and end-to-end distance, R, plotted against chain length (expressed as n-mer number) for the four PS molecules studied. See Figure 12.

chain length, $6S_N$ should be less than C_N.[14,15] This is observed in Figures 12−14. It can be seen that in all of the cases convergence to high molecular weight behavior is not achieved in the chain length ranges studied.

Reported[16,17] experimental limiting values of C_N are 6.7 and 7.3 for PE, 6.6 and 6.7 for PIB, and 10.0 and 9.5 for PS. In each case, the first value is from ref 16 and the second from ref 17. The simulation results appear to be reasonably consistent with these values. PE is probably in good agreement when allowance is made for the low temperature of the simulation in comparison with the experiments (in the melt or in solution above 400 K). That is, PE has a substantial negative temperature coefficient for C_N ($\sim 1 \times 10^{-3}$ K^{-1})[14] so that 300 K values of C_N should be in the vicinity of 8.0. The PIB values for $\langle R^2 \rangle$ are not very well converged statistically, especially at the higher values of N. As mentioned above, the end-to-end distances, R, are much noiser statistically than the radii of gyration. This is evident in Figure 13 for PIB, where the error bars represent the standard deviation of five equal subtrajectories out of the complete trajectory. However, the C_N value for PIB does appear to overshoot somewhat. PS may be a bit too high in the limit as well.

Comparison with Experiment. It is appropriate to briefly recapitulate the experiments reported by Chance et al.[3] The work included determination of elution or retention times of a large number of oligomers of PS, PIB, and PE. For many of these, independent values of molecular weight were available or were experimentally determined. At the lower molecular weights, individual oligomers of known degree of polymerization (DP) could be resolved. This circumstance allowed direct association of molecular weight with elution time without separate molecular weight measurement. The oligomers were studied on two column sets. One of these was a high-resolution column where long elution times necessary for resolution of the lower molecular weights could be obtained and the other was a so-called "linear" column which contained particles with pores of various diameters. Intrinsic viscosities of the oligomers were carefully determined. For PS, a wide range of experimental R_g values were available. Several R_g values were experimentally determined for PIB and were supplemented with values calculated from rotational isomeric state (RIS) theory. For PE, the R_g

values were from RIS calculations. The analysis below is based on the high resolution column results.

The UC method is based on the assumptions (1) that polymers with the same hydrodynamic radius and therefore for linear polymers the same value of R_g elute at the same time and (2) that values of R_g relative to the standard PS can be determined from the relation[14,18] relating intrinsic viscosity $[\eta]$ to the radius of gyration R_g and molecular weight, M, via a universal constant Φ as

$$[\eta] = \Phi\langle R_g^2\rangle^{3/2}/M \qquad (11)$$

Chance et al.[3] summarized their findings as follows. They discussed the validity of the above two assumptions in concert as expressed by eq 11. According to eq 11, the product $[\eta]M$ defines the radius of gyration, and thus polymers with the same $[\eta]M$ product should have the same elution time. If the product $[\eta]M$ is designated as the hydrodynamic volume, V_h, plots of V_h vs elution time for various polymer series should fall on the same curve. Actually, however, the plots of V_h where $[\eta]$ and M were experimentally determined independently showed significant differences among the PS, PIB, and PE series.[3] The R_g assumption was also tested separately. Plots of independently determined R_g values vs measured elution times were made. Again, all the polymers should fall on the same curve. The differences between the series were less but it was observed that significant differences still existed.

In the present work the same procedure is followed. The R_g vs elution time plots are presented again but modified to show the simulation results. In the previous work most of the samples of PS were polymerized by initiation with *n*-butyllithium, which places an *n*-butyl group at the start of the chain. The simulations were carried out on H-ended PS chains. PS chains terminated with H can be prepared by free-radical initiation.[3] Some retention time data for such chains are now included. The R_g values for PIB and PE at low molecular weight used previously[3] were from rotational isomeric state (RIS) calculations. The MD values determined here for PIB are systematically higher than the previous RIS values. These differences are probably, at least in part, due to fact that in the RIS calculations the mass is considered to be entirely concentrated at the main-chain atoms whereas in the MD calculations the mass is computed as distributed over all of the explicit atom centers including pendant side groups. For PS, Chance et al.[3] used only experimental values.

Since accurate plots of experimental retention times against independently determined molecular weight, usually assigned from individually resolved oligomers, are available as described above and the MD R_g values are known as a function of molecular weight, it is straightforward to construct a MD R_g vs retention time plot. In Figure 15 such plots, using the present MD values for R_g and labeled "R_g MD", are presented. If the R_g hypothesis held strictly, the plots of the three series would superpose. It may be seen that this is not the case.

In order to place the $[\eta]M$ product hypothesis results on the same plot as the R_g plots, the hydrodynamic volume, $V_h = [\eta]M$, is converted to a molecular radius which is designated as R_v[14] to distinguish it from direct R_g values. Thus

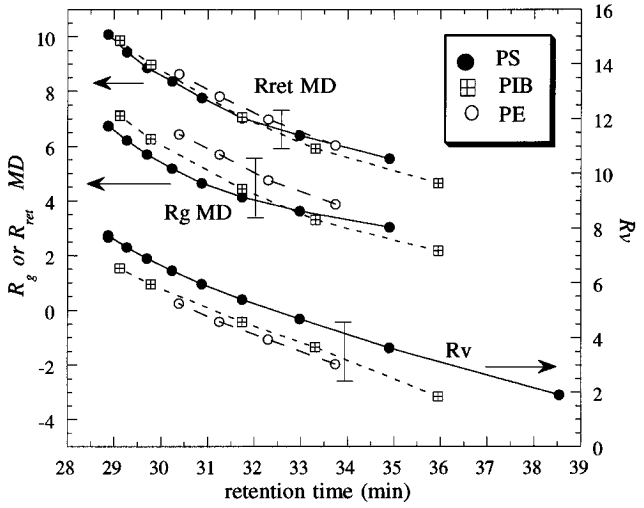

Figure 15. Three measures of molecular size vs experimental elution times for PS, PIB, and PE. The points labeled "R_v" are radii inferred from the intrinsic viscosity−molecular weight product, $[\eta]M$. The points labeled "R_g MD" are radii of gyration calculated directly in the MD simulations. The points labeled "R_{ret} MD" are retention radii as defined in the text and are determined from the MD simulations.

$$R_v = 2.5([\eta]M)^{1/3} \qquad (12)$$

when the units of $[\eta]$ are dL/g and R_g is in Å.[14] Plots of R_v vs retention time are also shown in Figure 15. Again the lack of a single superposed curve is apparent.

Most importantly in the context of the simulations is the effectiveness of the retention radius, R_{ret}, from simulation, as a criterion for elution behavior. It is defined above through eq 8 as an effective hard-sphere radius that reproduces the partition coefficients determined from simulation. Plots of MD R_{ret} values against retention time can be constructed in the same fashion as for the MD-determined R_g vs retention time plots of Figure 15. That is, the plots of experimental retention times against independently determined molecular weight are combined with the R_{ret} vs molecular weight plots to generate the desired R_{ret} vs retention time plots. These are also shown in Figure 15. It may be seen that the three polymer types are now much more closely grouped under the R_{ret} parameter as a measure of effective size in elution. Presumably, R_{ref} appears larger than "R_g MD", as it includes a van der Waals radius not in "R_g MD".

Chance et al.[3] also discussed the apparent molecular weights of oligomers obtained through the use of UC in SEC in comparison with the correct values. This is done here as well. The values of R_v that are plotted against elution time in Figure 15 can also be plotted against the independently determined or "true" molecular weights, M. For a given elution time a R_v value on the PIB or PE curves from Figure 15 thus leads to a "true" molecular weight, M_{true}, for that polymer. However, if the PS R_v vs elution time curve is used to determine R_v for the PIB or PE sample and this value is reduced to a molecular weight on the true R_v vs M curve for PIB or PE, this leads to a UC "predicted" value for the molecular weight, $M_{predicted}$. The ratio $M_{predicted}/M_{true}$ found in this manner is plotted in Figure 16 against M_{true} and shown as the "R_v" points. The procedure was also employed for the R_g values determined from MD simulation in this paper and for the retention radii R_{ret}. These $M_{predicted}/M_{true}$ values are designated as "R_g MD" and "R_{ret} MD", respectively, and are shown in Figure

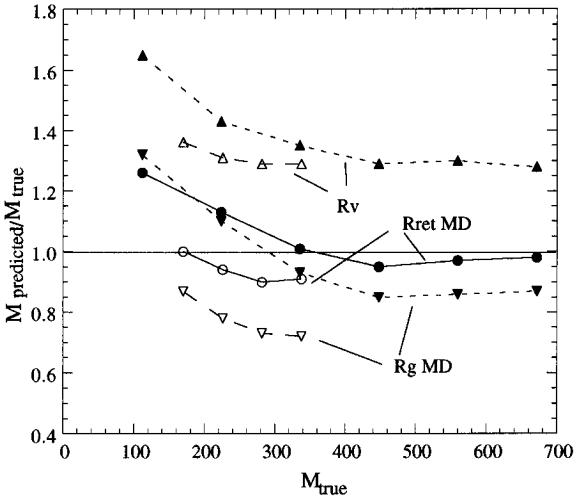

Figure 16. Accuracy of molecular weights, expressed as $M_{predicted}/M_{true}$, for PIB (filled symbols) and PE (open symbols) using PS as a standard. Three criteria for the elution time being the same as the standard are shown. The "R_v" points are for the UC criterion of the viscosity−molecular weight product, $[\eta]M$. The "R_g MD" points use the radius of gyration, R_g determined in MD simulations. The "R_{ret} MD" points use the retention radius determined in the MD simulations.

Table 3. Statistical Analysis of Molecular Weight Prediction Methods Using Polystyrene as a Standard Expressed as the Mean and Standard Error of $(M_{predicted}/M_{true} - 1)^2$

	universal calibration		R_g		R_{ret}	
polymer	mean	std error	mean	std error	mean	std error
PE	0.098	0.01	0.05	0.014	0.005	0.002
PIB	0.16	0.05	0.03	0.015	0.015	0.001

16. Since the MD R_g values are not the same as those used in ref 3 and the H end group is different, the previous figure of this type and Figure 16 here are not exactly the same. Obviously, the R_{ret} method results are entirely new. The magnitude of the error in the UC process depends on how the data are used. In Chance et al.[3] the $[\eta]M$ product was divided by the known $[\eta]$ for the tested polymer. The entire error in the polymer's $[\eta]M$ mismatch directly affected the evaluated molecular weight to the first power; call that result M_{1p}. In this paper the process of calculating R_v, done to make the process for the three radii equivalent, reduces the error by a fractional power; call that result M_{2p}. If an $[\eta] = KM^a$ type Mark−Houwink relationship is employed for the polymer, the error is reduced as the $1/(1 + a)$th root. Thus $M_{2p} = (M_{1p}/M_{true})^{1/(1+a)}$.[19]

It may be seen in Figure 16 that the use of directly determined radius of gyration rather than that inferred from the $[\eta]M$ product in eq 12, i.e, the "R_g MD" points vs the "R_v" points, gives better results for the molecular weight. This is similar to the previous conclusion.[3] However, it is also seen in Figure 16 that invoking equal retention radii, R_{ret}, i.e., the "R_{ret} MD" points, as the criterion for equal elution times improves the situation further.

All three of the above types of $M_{predicted}/M_{true}$ behavior for PIB and PE were subjected to a simple statistical analysis. The results for the deviation from unity, $(M_{predicted}/M_{true} - 1)^2$, are shown in Table 3. It is clear that both the means and standard errors of the measured statistic are smallest for the calibration based on R_{ret}, R_g MD is next best, and the R_v from UC is worst.

The fit using R_{ret} is poorest at the lowest M values. Perhaps this is not surprising since the simplifications of the simulation model could become relatively more serious for small molecules. These would include the elimination of solvent and interaction with the wall. Another related factor may simply be the basing of the R_{ret} values on the 50 Å pore diameter. This single simple parameter works surprisingly well. However, it may be based on too large a diameter to capture the geometric effects of the smallest molecules, i.e., in the dimer and trimer range. In any event, the effects at the smallest sizes seem to warrant further investigation. Preliminary results indicate that a 15 Å pore criterion improves the results at low molecular weight but at the expense of those at high. Perhaps a distribution of pore sizes is indicated.

In overall conclusion it can be said that sizes and geometries of polymers in the oligomer range as determined via MD simulation go a long way in rationalizing their behavior in size exclusion chromatography. Although radius of gyration is a better measure of the elution behavior than the hydrodynamic volume ($[\eta]M$), it is not the most effective measure in monitoring exclusion when the molecules are relatively short.

References and Notes

(1) Booth, C.; Price, C., Eds. *Comprehensive Polymer Science, Polymer Characterization*; Pergamon Press: New York, 1989; Vol. 1.
(2) Barth, H.; Mays, J., Eds. *Modern Methods of Polymer Characterization*; Wiley: New York, 1991.
(3) Chance, R. R.; Baniukiewicz, S. P.; Mintz, D.; Ver Strate, G.; Hadjichristidis, N. *Int. J. Polym. Charact. Anal.* **1995**, *1*, 1.
(4) Casassa, E. F. *J. Polym. Sci., Part B* **1967**, *5*, 773.
(5) Giddings, J. C.; Kucera, E.; Russell, C. P.; Meyers, M. N. *J. Phys. Chem.* **1968**, *72*, 14.
(6) Davidson, M. G.; Suter, U. W.; Deen, W. M. *Macromolecules* **1987**, *20*, 1141.
(7) Pant, P. V. K.; Boyd, R. H. *Macromolecules* **1993**, *26*, 679.
(8) Boyd, R. H.; Gee, R. H.; Han, J.; Jin, Y. *J. Chem. Phys.* **1994**, *101*, 788.
(9) Gee, R. H.; Boyd, R. H. *J. Chem. Phys.* **1994**, *101*, 8028.
(10) Sorensen, R. A.; Liau, W. B.; Kesner, L.; Boyd, R. H. *Macromolecules* **1988**, *21*, 200.
(11) Boyd, R. H.; Breitling, S. M.; Mansfield, M. L. *AIChE J.* **1973**, *19*, 1016. These parameters are available in the POLYMER module in the SYBYL simulation software of the Tripos Co., St. Louis, MO.
(12) Nosé, S. *J. Chem. Phys.* **1984**, *81*, 511.
(13) Einaga, Y.; Koyama, H.; Konishi, T.; Yamakawa, H. *Macromolecules* **1989**, *22*, 3419.
(14) Davidson, N. S.; Fetters, L. J.; Funk, W. G.; Hadjichristidis, N.; Graessley, W. W. *Macromolecules* **1987**, *20*, 2614.
(15) Boyd, R. H.; Phillips, P. J. *The Science of Polymer Molecules*; Cambridge University Press: Cambridge, 1993.
(16) Tabulated in Table I, Chapter II in ref 14.
(17) Fetters, L. J.; Lohse, D. J.; Richter, D.; Witten, T. A.; Zirkel, A. *Macromolecules* **1994**, *27*, 4639.
(18) Flory, P. J. *Principles of Polymer Chemistry*; Cornell University Press: Ithaca, NY, 1953.
(19) Manuscript in preparation.

MA9508663